

International Journal of Humanoid Robotics
© World Scientific Publishing Company

Passive Dynamic Autonomous Control of Bipedal Walking

Masahiro Doi

*Department of Micro-Nano System Engineering, Nagoya University
Furo-cho 1, Chikusa-ku, Nagoya, 464-8603, JAPAN
doi@robo.mein.nagoya-u.ac.jp*

Yasuhisa Hasegawa

*Institute of Engineering Mechanics and Systems, University of Tsukuba
Tennodai 1-1-1, Tsukuba, Ibaraki, 305-8573, JAPAN
hase@esys.tsukuba.ac.jp*

Toshio Fukuda

*Department of Micro-Nano System Engineering, Nagoya University
Furo-cho 1, Chikusa-ku, Nagoya, 464-8603, JAPAN
fukuda@robo.mein.nagoya-u.ac.jp*

Received (Day Month Year)

Revised (Day Month Year)

Accepted (Day Month Year)

This paper proposes the novel control method named Passive Dynamic Autonomous Control. PDAC is based on the following concept which Grizzle *et al.*¹⁰ used previously: 1) point-contact 2) interlocking. Point-contact means that the contact state between a robot and the ground is made point. This makes it possible to control based on the robot inherent dynamics although the control becomes difficult. Interlocking means that all robot joints are connected and interlocked. We present the new approach using this concept to describe the robot dynamics as a 1-DOF autonomous system. Due to autonomy, this approach has two following notable point: 1) period from foot-contact to next foot-contact can be obtained 2) there is a conservative quantity. In this paper, the coupling method of the sagittal and lateral motion that takes advantage of point 1 is proposed. In addition, the stabilizing method based on the conservative quantity is designed. By means of PDAC and these methods, stable 3-dimensional walking based on the robot inherent dynamics is realized.

Keywords: biped locomotion; dynamics; robotics.

1. Introduction

In the age of an aging society, the prospective role of robots is turning gradually from just working machines to do monotonous work in a factories to partners who support human life. In recent years, a lot of autonomous humanoid robots have been actually realized¹¹. These robots can walk on two legs stably by means of the control based on ZMP (Zero Moment Point). ZMP⁵, the indicator of the stability

of biped walking, is a point on the floor where the torque generated by both inertial and gravitational forces becomes zero. That is, using ZMP-based control to realize stable walking makes sense, thus a number of researches of ZMP-based control have been presented^{4,6}. However, in order to realize a partner robot, the robots controlled based on ZMP have a problem in terms of the run-time of the battery since ZMP-based method does not take advantage of the robot inherent dynamics.

To solve this problem, it is necessary to develop the dynamics-based method. Some researchers proposed the method to use the robot dynamics directly by making the point-contact between a robot and the ground^{2,3,15,17}. Miura and Shimoyama⁹ presented stilt-like biped and control method to stabilize the gaits by changing the robot posture at foot-contact. Kajita *et al.*¹² proposed the control method based on the conserved quantity introduced due to a horizontal COG (Center Of Gravity) trajectory. Goswami *et al.*^{1,16} reported the method to realize quasi-passive walking on the horizontal ground. Grizzle and Westervelt *et al.*^{10,14,13} proposed the control method of the underactuated planar robot with a trunk and proved its stability. Although some of these point-contact methods actually realized smooth dynamic walking, their walking was 2-dimensional or that of a robot without trunk. Thus, the main goal of this paper is to propose the new control method based on the point-contact and realize 3-dimensional dynamic walking of a multiple link robot with a trunk.

In this paper, we propose the novel control method named Passive Dynamic Autonomous Control (PDAC). PDAC assumes two following premises: 1) point-contact 2) interlocking. The second premise means that the angles of robot joints are connected with the angle around contact point. Although since this concept was proposed first by Grizzle *et al.*¹⁰, it was not original of this paper, we propose the new method to control the robot dynamics by means of it. The approach of PDAC is to describe the robot dynamics as a 1-DOF autonomous system, which is the dynamics around contact point. This approach makes it possible to calculate the period from foot-contact to next foot-contact (we term this foot-contact period hereinafter), hence the foot-contact period of the lateral motion and that of the sagittal one can be made identical. In this paper, on the assumption that the sagittal and lateral motion can be separated, each motion is designed by means of PDAC. Then, by keeping the conservative quantity of the autonomous system, the walking motion is stabilized. In addition, we propose coupling method of each motion to make the each foot-contact period identical. Finally, by means of the proposed method, 3-dimensional natural dynamic walking based on the robot inherent dynamics is realized.

In section 2, PDAC is explained in detail and in section 3, the 3-dimensional walking is designed by means of PDAC. Section 4 describes the experiment of proposed method. Lastly, section 5 is conclusion.

2. Passive Dynamic Autonomous Control

2.1. Target Dynamics

The concept of PDAC is the same as that Grizzle *et al.*¹⁰ proposed before. We begin with the two following premises. First, the contact state between a robot and the ground is point-contact. Second, robot joints are interlocked with the angle around the contact point. The first premise means that the first joint of a robot, i.e. the ankle joint of the stance leg, is passive. The second means that the angles of active joints are described as the function of the angle around the contact point. Assuming that PDAC is applied to the serial n-link rigid robot shown in Fig. 1, these two premises are expressed as follows:

$$\tau_1 = 0 \quad (1)$$

$$\Theta = [\theta_1, \theta_2, \dots, \theta_n]^T = [f_1(\theta), f_2(\theta), \dots, f_n(\theta)]^T = \mathbf{f}(\theta) \quad (2)$$

where θ is the angle around the contact point in the absolute coordinate system. Since it has no effect on the robot dynamics due to point-contact, the level ground is assumed, therefore $\theta_1 = f_1(\theta) = \theta$.

The dynamic equations of this model are given by

$$\frac{d}{dt} \left(M(\Theta) \dot{\Theta} \right) - \frac{1}{2} \frac{\partial}{\partial \Theta} \left(\dot{\Theta}^T M(\Theta) \dot{\Theta} \right) - G(\Theta) = \tau \quad (3)$$

where $M(\Theta) = [M_1(\Theta), M_2(\Theta), \dots, M_n(\Theta)]^T$, $\Theta = [\theta_1, \theta_2, \dots, \theta_n]^T$, $G(\Theta) = [G_1(\Theta), G_2(\Theta), \dots, G_n(\Theta)]^T$, $\tau = [\tau_1, \tau_2, \dots, \tau_n]^T$, $\frac{\partial}{\partial \Theta} = \left[\frac{\partial}{\partial \theta_1}, \frac{\partial}{\partial \theta_2}, \dots, \frac{\partial}{\partial \theta_n} \right]^T$. Since in this model the dynamic equation around the contact point has no term of

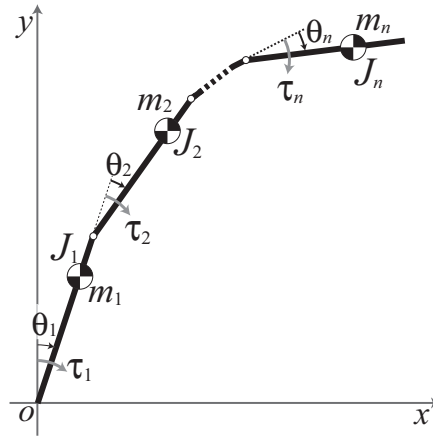


Fig. 1. Mechanical model of the serial n-link rigid robot. θ_i and τ_i are the angle and the torque of i th joint respectively. m_i and J_i are the mass and the moment of inertia of i th link respectively.

4 Masahiro Doi, Yasuhisa Hasegawa, Toshio Fukuda

the Coriolis force, it is given as

$$\frac{d}{dt} \left(\mathbf{M}_1(\Theta) \dot{\Theta} \right) - G_1(\Theta) = \tau_1 \quad (4)$$

By differentiating Eq. (2) with respect to time, the following equation is acquired,

$$\dot{\Theta} = \frac{\partial \mathbf{f}(\theta)}{\partial \theta} \dot{\theta} = \left[\frac{\partial f_1(\theta)}{\partial \theta}, \frac{\partial f_2(\theta)}{\partial \theta}, \dots, \frac{\partial f_n(\theta)}{\partial \theta} \right]^T \dot{\theta}. \quad (5)$$

Substituting Eq. (1), (2) and (5) into Eq. (3) yields the following dynamic equation,

$$\frac{d}{dt} \left(M(\theta) \dot{\theta} \right) = G(\theta) \quad (6)$$

where

$$M(\theta) := \mathbf{M}_1 \left(\mathbf{f}(\theta) \right) \frac{d\mathbf{f}(\theta)}{d\theta} \quad (7)$$

$$G(\theta) := G_1 \left(\mathbf{f}(\theta) \right). \quad (8)$$

By multiplying both sides of Eq. (6) by $M(\theta)\dot{\theta}$ and integrating with respect to time, the dynamics around the contact point is obtained as follows:

$$\int \left(M(\theta) \dot{\theta} \right) \frac{d}{dt} \left(M(\theta) \dot{\theta} \right) dt = \int M(\theta) G(\theta) \dot{\theta} dt \quad (9)$$

$$\Leftrightarrow \dot{\theta} = \frac{1}{M(\theta)} \sqrt{\int 2G(\theta)M(\theta) d\theta}. \quad (10)$$

Assuming that the integration in right side of Eq. (10) is calculated as $\int G(\theta)M(\theta) d\theta = D(\theta) + C$, Eq. (10) is described as the following 1-DOF autonomous system,

$$\dot{\theta} = \frac{1}{M(\theta)} \sqrt{2(D(\theta) + C)} \quad (11)$$

$$:= F(\theta). \quad (12)$$

In this paper, we term Eq. (11) and (12) target dynamics.

2.2. Dynamics Interlocking

As mentioned previously, PDAC is based on the two premises: passivity and interlocking. These premises make it possible to describe the whole robot dynamics as the 1-DOF autonomous system, owing to which the simple and valid controller based on the robot dynamics can be composed. However, interlocking of joint angles has possibility to bring about the problem that the robot vibrates and the controller loses its stability during locomotion, especially at foot-contact, since if the passive joint vibrates, all of other active joints also do. In order to solve this problem, all of robot joints are controlled according to the desired dynamics of each joint derived from the interlocking function Eq. (2) and the target dynamics Eq. (12) as follows:

$$\dot{\theta}_i = \frac{\partial f_i}{\partial \theta} F(f_i^{-1}(\theta_i)) \quad (i = 1, 2, 3, \dots). \quad (13)$$

These desired dynamics are independent from each other, thus it is necessary to connect the desired dynamics of active joints with the target dynamics in order to prevent the whole walking motion being broken in case of the error between the target dynamics and the actual dynamics of θ . Hence, we define the connection between the target dynamics and the active joints. The controller decides the desired angular velocities of each joint as described below,

$$\dot{\theta}_1^d = F(f_1^{-1}(\theta_1)) \quad (14)$$

$$\dot{\theta}_i^d = \frac{\partial f_i}{\partial \theta} F(f_i^{-1}(\theta_i)) + k_i(f_i(\theta) - \theta_i) \quad (i = 2, 3, \dots) \quad (15)$$

$$\iff \dot{\Theta}^d := \mathbf{F}(\Theta) \quad (16)$$

where k_i is the strength of connection determined experimentally since its value has little effect on the robot dynamics. As for humanoid robots, the ground slope at the contact point is deduced from the angle of the ankle joint of the swing leg at foot-contact, and θ is calculated from θ_1 and the ground slope. The remarkable point is that if there is no error such as the model error or disturbance, the second term of Eq. (15) is constantly zero and the actual dynamics of θ is identical with the target dynamics definitely.

Fig. 2 shows the block diagram of PDAC of bipedal locomotion. The control loop including a robot (enclosed by the dotted line in Fig. 2) have no input, thus it can be considered that the control system is autonomous. This autonomy makes it possible to realize the natural dynamic motion based on the inherent dynamics of a robot. The loop described by the broken line is executed only at the moment of foot-contact. In this loop, the target dynamics of next step is determined according to both the desired parameters such as walking velocity and the robot status, then \mathbf{F} is updated. Since this updating compensates the error between the previous target dynamics and the actual ones around the contact point, it is possible to realize stable walking.

2.3. PDAC Constant

Since as mentioned previously, the target dynamics is autonomous, in addition, independent of time, it is considered as a kind of conservative system. Therefore, it is conceivable that the target dynamics has a conserved quantity. As for PDAC, it is the constant of integration in right side of Eq. (10). That is, C in Eq. (11) is the conserved quantity of the target dynamics, which is named PDAC Constant. It is clear that PDAC Constant is decided in accordance with initial condition and that the robot motion is generated as it is kept constant. In order to stabilize walking, the controller updates the target dynamics according to PDAC Constant. This method to update is presented later.

6 Masahiro Doi, Yasuhisa Hasegawa, Toshio Fukuda

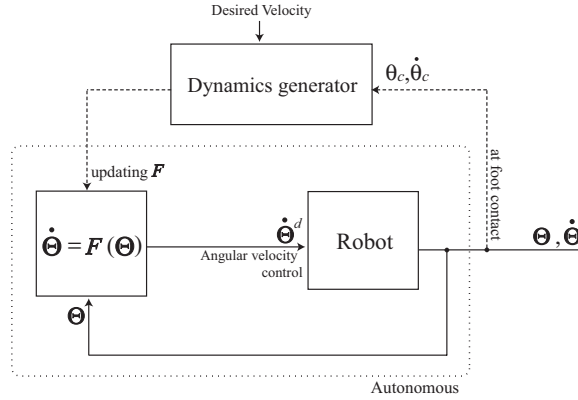


Fig. 2. Block diagram of PDAC of bipedal locomotion. θ_c and $\dot{\theta}_c$ are the angle and the angular velocity of θ_1 at foot-contact respectively.

3. Bipedal Walking Control

In this paper, it is assumed that lateral motion and sagittal one can be separated and controlled independently since lateral side-to-side rocking motion is quite small and step-length in the sagittal plane is relatively short. Although both motions are composed independently, the period from foot-contact to next foot-contact (foot-contact period) in the both plane are necessary to be identical. We design each motion by means of PDAC by giving both the desired step-length, λ^d , and desired foot-contact period, T^d , and propose the coupling method of both motions. In addition, the landing position control is designed based on PDAC. At first the sagittal motion control is presented, followed by the lateral motion control satisfying the condition of the foot-contact period is explained.

3.1. Sagittal motion control

3.1.1. 3-link model

For the sake of simplicity, the 3-link model as shown in Fig. 3 is used in this paper, i.e. upper body of robot is not moved. Although how to interlock might affect the whole robot dynamics and its motion, the easiest interlocking is applied in this paper. Similarly, we do not treat the effect of upper body motion on the robot dynamics by locking it. Both effects on the robot dynamics are not clarified in this paper and future works. The dynamic equation of this model is described as Eq. (3) and that of the ankle joint of the stance leg is Eq. (4) where $n = 3$. The left side of

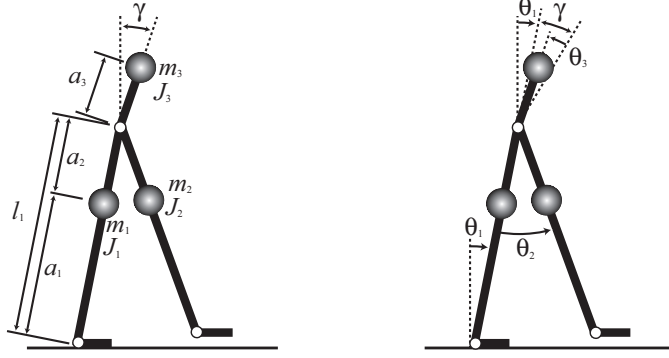


Fig. 3. 3-link model in the sagittal plane. m_i , J_i , l_i and a_i are the mass, the moment of inertia, the length of link and the distance from the joint to the link COG of link i respectively. γ is the angle of the forward tilting. In the right figure, θ_1 , θ_2 and θ_3 are the ankle angle of the stance leg, the angle from the stance leg to the the swing leg, the angle to swing the trunk up respectively.

Eq. (4) is described as follows:

$$M_{11}(\Theta) = J_1 + J_2 + J_3 + m_1 a_1^2 + m_2 l_1^2 + m_2 a_2^2 - 2m_2 a_2 l_1 \cos \theta_2 + m_3 l_1^2 + m_3 a_3^2 + 2m_3 a_3 l_1 \cos(\gamma - \theta_3) \quad (17)$$

$$M_{12}(\Theta) = -J_2 - m_2 a_2^2 + m_2 a_2 l_1 \cos \theta_2 \quad (18)$$

$$M_{13}(\Theta) = -J_3 - m_3 a_3^2 - m_3 a_3 l_1 \cos(\gamma - \theta_3) \quad (19)$$

$$G_1(\Theta) = (m_1 a_1 + m_2 l_1 + m_3 l_1) g \sin \theta_1 + m_2 g a_2 \sin(\theta_2 - \theta_1) + m_3 g a_3 \sin(\theta_1 + \gamma - \theta_3) \quad (20)$$

where $\mathbf{M}_1(\Theta) = [M_{11}(\Theta), M_{12}(\Theta), M_{13}(\Theta)]$.

3.1.2. Interlocking of sagittal joints

Grizzle *et al.*¹⁰ used the following interlocking in their previous paper: to maintain the angle of the torso at some constant value and to command the swing leg to behave as the mirror image of the stance leg. In this paper, we use the same interlocking, that is,

$$\theta_1 = f_1(\theta) = \theta - \beta \quad (21)$$

$$\theta_2 = f_2(\theta) = 2\theta \quad (22)$$

$$\theta_3 = f_3(\theta) = \theta \quad (23)$$

8 Masahiro Doi, Yasuhisa Hasegawa, Toshio Fukuda

where β is the ground slope at the contact point (ascent is positive). From Eq. (21)-(23) and (1), Eq. (6) is

$$M_s(\theta) = (J_1 - J_2 + m_1 a_1^2 + m_2 l_1^2 - m_2 a_2^2 + m_3 l_1^2) + m_3 a_3 l_1 \cos(\gamma - \theta) \quad (24)$$

$$:= E_1 + E_2 \cos(\gamma - \theta) \quad (25)$$

$$G_s(\theta) = (m_1 a_1 + m_2 l_1 + m_2 a_2 + m_3 l_1)g \sin \theta + m_3 g a_3 \sin \gamma \quad (26)$$

$$:= E_3 + E_4 \sin \theta. \quad (27)$$

Thus,

$$\int M_s(\theta)G_s(\theta)d\theta = \int (E_1 + E_2 \cos(\gamma - \theta))(E_3 + E_4 \sin \theta)d\theta \quad (28)$$

$$= E_2 E_4 \left(\frac{\sin(\gamma\theta)}{2} - \frac{\cos(2\theta - \gamma)}{4} \right) + E_2 E_3 \sin(\theta - \gamma) - E_1 E_4 \cos \theta + E_1 E_3 \theta + C_s \quad (29)$$

$$:= D_s(\theta) + C_s \quad (30)$$

where C_s is the integral constant, which is PDAC Constant of the sagittal motion. From Eq. (11), the target dynamics in the sagittal plane is

$$\dot{\theta} = \frac{1}{M_s(\theta)} \sqrt{2(D_s(\theta) + C_s)} \quad (31)$$

$$:= F_s(\theta). \quad (32)$$

From Eq. (21)-(23), $f_1^{-1}(\theta_1) = \theta_1 + \beta$, $f_2^{-1}(\theta_2) = \frac{1}{2}\theta_2$, $f_3^{-1}(\theta_3) = \theta_3$ are obtained, thus the desired angular velocity of sagittal joints are described as follows:

$$\dot{\theta}_1^d = F_s(\theta_1 + \beta) \quad (33)$$

$$\dot{\theta}_2^d = 2F_s\left(\frac{\theta_2}{2}\right) + k_2(2\theta - \theta_2) \quad (34)$$

$$\dot{\theta}_3^d = F_s(\theta_3) + k_3(\theta - \theta_3). \quad (35)$$

3.1.3. Foot contact model

In this paper, it is assumed that foot-contact is occurred for a moment and the angular momentum around the contact point is valied instantly. The angular momentum is described as

$$P = M_s(\theta)\dot{\theta}. \quad (36)$$

Fig. 4 depicts some parameters at foot-contact. Assuming that the translational velocity along the pendulum at foot-contact is zero since it is quite small, the angular velocity around the contact point is acquired as follows:

$$l^+ P^+ = l^- P^- \cos(\xi^- + \xi^+) \quad (37)$$

$$\iff {}_i\dot{\theta}^+ = \frac{l^- M_s({}_i\theta^-)}{l^+ M_s({}_i\theta^+)} \cos(\xi^- + \xi^+) {}_i\dot{\theta}^- \quad (38)$$

$$\iff {}_i\dot{\theta}^+ := H_s {}_i\dot{\theta}^- \quad (39)$$

From this value, PDAC Constant at the i th step, ${}_iC_s$, is obtained as below,

$${}_iC_s = \frac{1}{2} \left(M_s ({}_i\theta^+) \dot{{}_i\theta}^+ \right)^2 - D_s ({}_i\theta^+). \quad (40)$$

3.1.4. Desired PDAC Constant

Since the target dynamics is the 1-DOF autonomous system, it is possible to calculate the foot-contact period by integrating Eq. (12) with respect to time. The foot-contact period satisfying the desired step-length is calculated as below:

$$\dot{\theta} = F_s(\theta) \quad (41)$$

$$\Leftrightarrow \frac{1}{F_s(\theta)} d\theta = dt \quad (42)$$

$$\Leftrightarrow \int_{{}_{i+1}\hat{\theta}^-}^{{}_i\hat{\theta}^+} \frac{1}{F_s(\theta)} d\theta = \hat{T}_s \quad (43)$$

where ${}_i\hat{\theta}^+ = {}_{i+1}\hat{\theta}^- = \sin^{-1} \frac{\lambda^d}{2l_1}$ are the desired value of ${}_i\theta^+$ and ${}_{i+1}\theta^-$ that can be calculated from desired step-length. This period is necessary to be identical with the desired foot-contact period, thus

$$\hat{T}_s = T^d. \quad (44)$$

In order to generate the stable cyclic walking, the angular velocity around the contact point after impact is necessary to be kept constant, that is,

$${}_i\dot{\theta}^+ = {}_{i+1}\dot{\theta}^+. \quad (45)$$

By solving two conditions, Eq. (44) and (45), by means of two dimensional approximation of ${}_i\hat{\theta}^+$ and ${}_{i+1}\hat{\theta}^-$, desired PDAC Constant is decided,

$$C_s^d = C_s^d(T^d, \lambda^d). \quad (46)$$

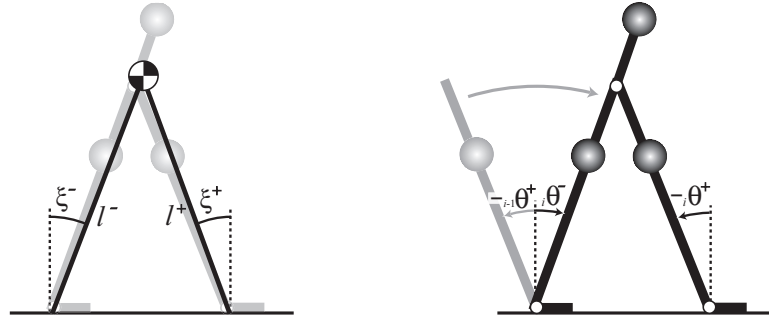


Fig. 4. Parameters at foot-contact. l^- and ξ^- are the length and inclination of the inverted pendulum which connects the supporting foot and the COG of the whole robot before impact, while l^+ and ξ^+ are those after impact. ${}_i\theta^-$ and ${}_i\theta^+$ are the angles around the contact point before and after impact of the i th step.

3.1.5. Stabilization of sagittal motion

Since the target dynamics is the conservative system, if PDAC Constant is kept constant, the stability of the motion is guaranteed. In order to stabilize walking, step-length is varied according to PDAC Constant. This method takes advantage of the loss of angular momentum at foot-contact, that is, if the step-length is long, the loss is high, while if short, it is low. The control strategy is to adjust the step-length of the next step after every foot-contact in accordance with the desired PDAC Constant and the actual one as follows:

$$\frac{C_s^d + D_s(i_{+1}\theta^+)}{M_s(i_{+1}\theta^+)^2} = \frac{D_s(i_{+1}\theta^-) + {}_iC_s}{M_s(i_{+1}\theta^-)^2} H_s^2 \quad (47)$$

$$\iff {}_{i+1}\theta^- = {}_{i+1}\theta^+ (C_s^d, {}_iC_s). \quad (48)$$

Note, however, that since in this paper the level ground is assumed, ${}_{i+1}\theta^- = {}_{i+1}\theta^+$.

This stabilizing control makes it possible to keep PDAC Constant in the vicinity of desired value. Therefore, sagittal motion is kept stable.

Here, the point to notice is that the foot-contact period differs from the desired foot-contact period due to stabilization. Hence, it is necessary to control the lateral motion so that the period of lateral motion is identical with the following period of sagittal motion,

$$T_s = \int_{{}_i\theta^+}^{{}_{i+1}\theta^-} \frac{1}{F_s(\theta)} d\theta. \quad (49)$$

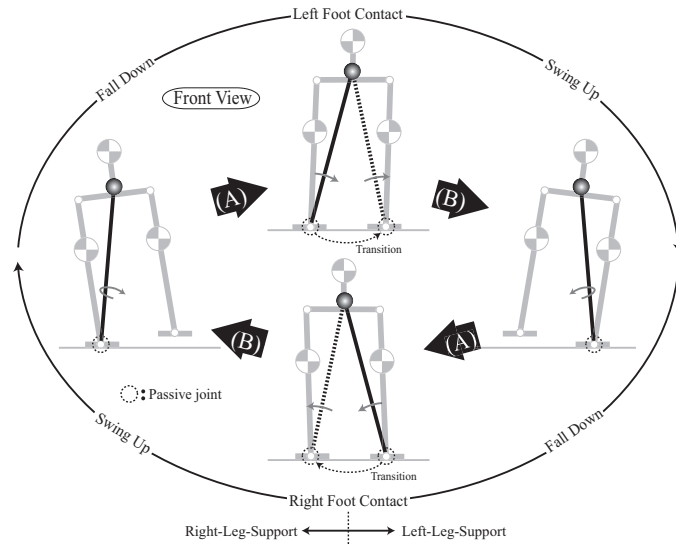


Fig. 5. The lateral motion of lateral-based walk (front view). The inverted pendulum falls off in phase(A) and swing up in phase(B)

3.2. Lateral motion control

3.2.1. Lateral motion

Many reserchers investigated and proposed the lateral motion control^{7,18,2}. In this paper, we design the lateral motion by means of PDAC as depicted in Fig. 5. In order to continue the side-to-side rocking motion, a robot lifts its pelvis in phase(A) and (B). The inverted pendulum whose length is variable is used as the model of the lateral plane since the motion to lift pelvis is quite small, in additon, a robot posture is valied little thus the motion to lift pelvis can be considered that to lengthen the pendulum. The lateral motion can be continued in spite of the loss of angular momentum at foot-contact by changing the pendulum length at impact.

3.2.2. Collision Inverted Pendulum Model

The following model shown in Fig. 6 is used as the model of the lateral motion: two inverted pendulums which are opposite each other continue to rock, iterating the collision between them, which is named Collision Inverted Pendulum Model (CIPM). This CIPM is intuitively like that the Newton's Pendulum is inverted. Fig. 7 shows the trajectory of COG and two coordinate systems Σ^R and Σ^L that correspond to right- and left-leg-support period respectively, and Fig. 7(b) depicts the phase portraits of ϕ^R and ϕ^L . These two phase portrait's coalescing yields the phase portrait of CIPM (see Fig. 7(c)). In the phase portrait of CIPM, there is the area in which has the circular nature between the coordinate systems Σ^R and Σ^L . In this area, the periodic motion can be realized due to the circular nature.

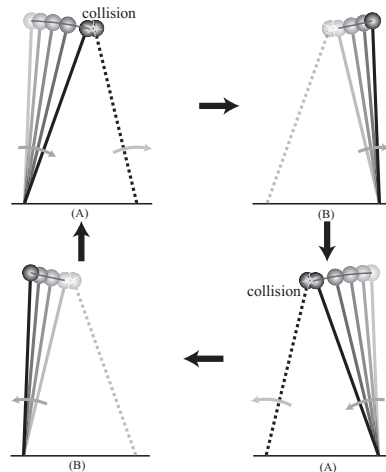


Fig. 6. Motion of CIPM. The collision between the foot and the ground is regarded as that between two pendulums. (A) and (B) correspond to those in Fig. 5.

12 Masahiro Doi, Yasuhisa Hasegawa, Toshio Fukuda

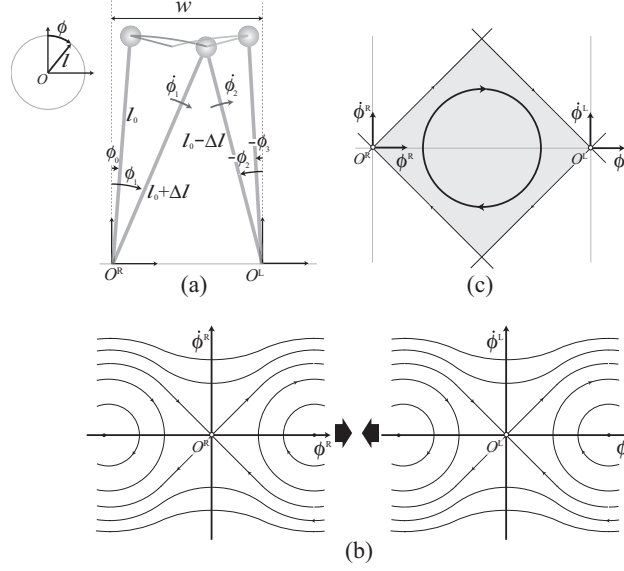


Fig. 7. (a) Trajectory of COG and polar coordinate systems Σ^R , Σ^L . l and ϕ denote the length and the angle of an inverted pendulum. (l_0, ϕ_0) and $(l_0 + \Delta l, \phi_1)$ are the coordinates in Σ^R at the beginning and ending of phase (A), $(l_0 - \Delta l, \phi_2)$ and (l_0, ϕ_3) is that of Σ^L of phase (B) respectively. $\dot{\phi}_1, \dot{\phi}_2$ denotes the angular velocity at the end of phase (A) and at the beginning of phase (B). (b) Phase portraits of ϕ^R and ϕ^L (c) Phase portrait of CIPM. The gray tetragon surrounded by the pair of separatrixes is named CIP-Area.

3.2.3. Interlocking of lateral joints

In this paper, the interlocking in the lateral plane is defined as below,

$$\text{Phase(A)} : l = f_A(\phi) = a_1\phi + b_1 \quad (50)$$

$$\text{Phase(B)} : l = f_B(\phi) = a_2\phi^2 + b_2\phi + c_2 \quad (51)$$

where,

$$a_1 = \frac{1}{\phi_1 - \phi_0} \Delta l \quad (52)$$

$$b_1 = l_0 - \frac{\phi_0}{\phi_1 - \phi_0} \Delta l \quad (53)$$

$$a_2 = \frac{1}{(\phi_3 - \phi_2)^2} \Delta l \quad (54)$$

$$b_2 = -\frac{2\phi_2}{(\phi_3 - \phi_2)^2} \Delta l \quad (55)$$

$$c_2 = l_0 - \frac{\phi_3^2 - 2\phi_2\phi_3}{(\phi_3 - \phi_2)^2} \Delta l. \quad (56)$$

l is the monotone increasing function of ϕ meeting the following conditions in phase (A): $f_A(\phi_0) = l_0$ and $f_A(\phi_1) = l_0 + \Delta l$, while in phase (B): $f_B(\phi_2) = l_0 - \Delta l$, $f'(\phi_2) = 0$ and $f(\phi_3) = l_0$.

The dynamic equation of the angle of an inverted pendulum is described as follows:

$$\frac{d}{dt} \left((ml^2 + J)\dot{\phi} \right) = mgl \sin \phi. \quad (57)$$

From the interlocking, Eq. (6) is described as follows:

$$M_{l_N}(\phi) = mf_N(\phi)^2 + J \quad (58)$$

$$G_{l_N}(\phi) = mgf_N(\phi) \sin \phi \quad (59)$$

where the suffix N means phase (N) (N=A, B). From Eq. (11), the target dynamics in the lateral plane is

$$\dot{\phi} = \frac{1}{M_{l_N}(\phi)} \sqrt{\int 2M_{l_N}(\phi)G_{l_N}(\phi) d\phi} \quad (60)$$

$$:= \frac{1}{M_{l_N}(\phi)} \sqrt{2(D_{l_N}(\phi) + C_{l_N})} \quad (61)$$

$$:= F_{l_N}(\phi) \quad (62)$$

where C_{l_N} is the integral constant, which is PDAC Constant of the lateral dynamics.

Assuming that the collision between the swing leg and the ground is perfectly non-elastic, the angular velocity of the inverted pendulum after impact is

$$\dot{\phi}_2 = \frac{v_1}{l_0 - \Delta l} \cos(\phi_1 - \phi_2 - \zeta) \quad (63)$$

$$= \frac{\sqrt{a_1^2 + (l + \Delta l)^2}}{l_0 - \Delta l} \cos(\phi_1 - \phi_2 - \zeta) \dot{\phi}_1 \quad (64)$$

$$:= H_l \dot{\phi}_1 \quad (65)$$

where

$$v_1 = \sqrt{(l\dot{\phi})^2 + \dot{l}^2} \Big|_{\phi=\phi_1} = \sqrt{a_1^2 + (l + \Delta l)^2} \dot{\phi} \quad (66)$$

$$\zeta = \tan^{-1} \left(\frac{\dot{l}}{l\dot{\phi}} \right) \Big|_{\phi=\phi_1} = \tan^{-1} \left(\frac{a_1}{l + \Delta l} \right). \quad (67)$$

Δl is the control value of the lateral motion. It is calculated from the condition of the beginning of phase(A) and the end of phase(B): $F_{l_A}(\phi_0) = 0$ and $F_{l_B}(\phi_3) = 0$. That is,

$$\frac{D_{l_A}(\phi_1) - D_{l_A}(\phi_0)}{M_{l_A}(\phi_1)^2} H_l^2 = \frac{D_{l_B}(\phi_3) - D_{l_B}(\phi_2)}{M_{l_B}(\phi_2)^2}. \quad (68)$$

Δl is so small that it can be obtained from this equation by means of liner approximation of Δl ,

$$\Delta l = \Delta l(\phi_0, \phi_3). \quad (69)$$

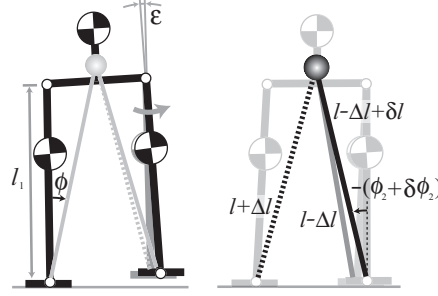


Fig. 8. Adjustment of foot width. ϵ is the angle to open the swing leg to adjust the foot width. $l - \Delta l + \delta l$ and $\phi_2 + \delta\phi_2$ are the pendulum length and angle at the beginning of phase (B) after adjustment.

Finally, it is necessary to determine the desired amplitude of the rocking motion, ϕ_0^d , so that the foot-contact period in the lateral plane matches with the desired foot-contact period. This condition is described as below,

$$\int_{\phi_0^d}^{\phi_1} \frac{1}{F_{l_A}(\phi)} d\phi + \int_{\phi_2}^{\phi_0^d} \frac{1}{F_{l_B}(\phi)} d\phi = T^d. \quad (70)$$

By means of two dimensional approximation of ϕ , it is possible to calculate ϕ_0^d from Eq. (70),

$$\phi_0^d = \phi_0^d(T^d). \quad (71)$$

By setting ϕ_3 at $-\phi_0^d$ at the beginning of phase (A) of every step, the lateral motion can be stabilized.

3.2.4. Coupling with the sagittal motion

As mentioned previously, it is necessary that the foot-contact period of the sagittal motion and that of the lateral motion are made identical. In case of the adjustment of step-length, the sagittal foot-contact period differs from the desired foot-contact period, thus the lateral motion needs to be varied according to the period of Eq. (49).

In order to control the lateral foot-contact period, the foot width is adjusted as shown in Fig. 8. $l - \Delta l + \delta l$ and $\phi_2 + \delta\phi_2$ are acquired from ϵ geometrically. It is assumed that this adjustment is so small that its effect on the target dynamics in phase (A) can be neglected. By the adjustment, the parameters of the target

dynamics in phase (B) is valied as follows:

$$a_2 = \frac{1}{(\phi_3 - (\phi_2 + \delta\phi_2))^2}(\Delta l - \delta l) \quad (72)$$

$$b_2 = -\frac{2\phi_2}{(\phi_3 - (\phi_2 + \delta\phi_2))^2}(\Delta l - \delta l) \quad (73)$$

$$c_2 = l_0 - \frac{\phi_3^2 - 2(\phi_2 + \delta\phi_2)\phi_3}{(\phi_3 - (\phi_2 + \delta\phi_2))^2}(\Delta l - \delta l). \quad (74)$$

The condition that the pendulum paused at the end of phase (B) is $F_{l_B}(\phi_3) = 0$, hence

$$D_{l_B}(\phi_3) - D_{l_B}(\phi_2 + \delta\phi_2) + \left(M(\phi_2 + \delta\phi_2)\dot{\phi}_2\right)^2 = 0. \quad (75)$$

In addition, the condition of the foot-contact period is necessary to be satisfied,

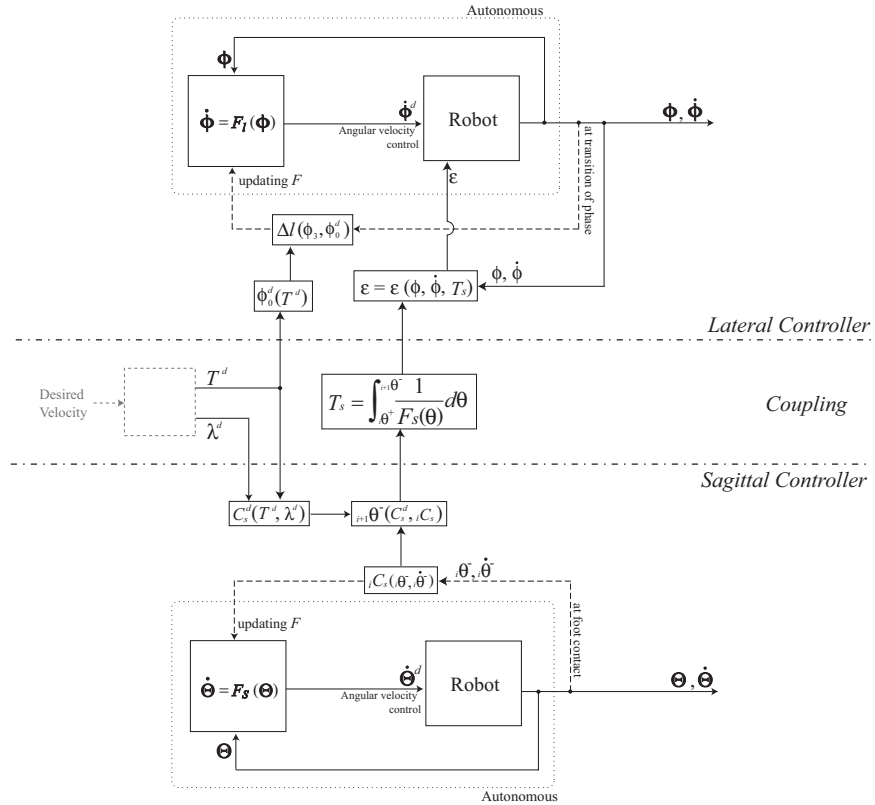


Fig. 9. Block diagram of the coupling between the sagittal and lateral motions

16 Masahiro Doi, Yasuhisa Hasegawa, Toshio Fukuda

namely,

$$\int_{\phi_2+\delta\phi_2}^{\phi_3} \frac{1}{F_{l_B}(\phi)} d\phi + \int_{\phi_3}^{\phi_1} \frac{1}{F_{l_A}(\phi)} d\phi = T_s. \quad (76)$$

The first term of the left side in Eq. (76) is the period of phase (B) and the second term is that of subsequent phase (A). Two conditions of Eq. (75) and (76) have two unknowns, i.e. the adjustment value, ϵ , and the pendulum angle at the end of phase (B), ϕ_3 . By solving these two conditions by means of linear approximation of ϵ and two dimensional approximation of ϕ_3 , the adjustment value, ϵ , can be calculated

$$\epsilon = \epsilon(\phi, \dot{\phi}, T_s). \quad (77)$$

3.3. Summary

Fig. 9 depicts the block diagram of the algorithm described in previous sections. At foot-contact, the sagittal controller decides the step-length, i.e. the value of θ at next foot-contact in order to stabilize the sagittal motion. Next, the foot-contact period of the sagittal motion is calculated by integration. Finally, the lateral controller determines the adjustment value of foot width according to both the sagittal foot-contact period and the present status in the lateral plane. This series of controls can be considered as the landing position control of three dimensional walking since the step-length is adjusted in the sagittal plane and the foot width is adjusted in the lateral plane.

The box enclosed by gray dashed line is the algorithm to decide the desired foot-contact period and step-length so that the energy consumption is minimized. However, this has not been solved and it's the future work, hence we give the desired foot-contact period and step-length to the controller directly in this paper.

4. Experiment

In this section, at first, the robot used in the experiment is mentioned, next, the experimental results are described.

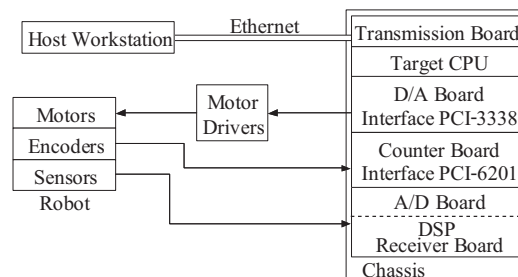


Fig. 10. Experimental setup

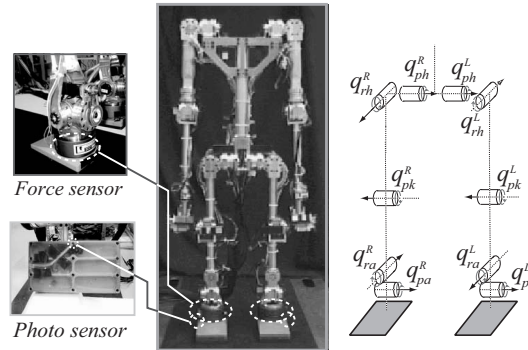


Fig. 11. Gorilla Robot II (about 1.0[m] height, 22.0[kg] weight, 24 DOF)

4.1. Experimental Setup

Fig. 10 depicts our experimental setup and Fig. 11 shows our robot “Gorilla Robot II”. This robot is driven by 24 AC motors of 20-30W with 100-200 times of speed reduction by harmonic gears. It has the following sensors: 1) encoders to get joint angles 2) force sensors to measure forces and moments to the foot 3) photo sensors to perceive foot-contact. The right in Fig. 11 shows the structure of its lower body.

4.2. Experimental results

The experiment of the walking proposed in the previous section on the flat and level ground was conducted. Since, in order to start the walking, the robot needs the potential energy, we lifted up the lateral pendulum to the position at the beginning of phase (A) and released. In experiment, the robot bends its knee joint of the swing leg so as to prevent the foot being in friction with the ground immediately after foot-contact on the assumption that the effect of knee bending on the robot dynamics can be neglected. The foot of the swing leg is actuated so as to be kept parallel to the ground.

The desired step-length is given to be gradually increased within initial 5 steps up to 0.15[m] and the desired foot-contact period is given at 0.7[s]. In consequence, the dynamic and natural walking is realized over 25 steps. The step-length is about 0.15[m] and the walking velocity is about 0.23[m/s]. Fig. 12 shows the snapshots of the PDAC walking at 1st, 7th, 12th, 16th, 19th, 22th step respectively. The angle and angular velocity of the lower body joints are depicted in Fig. 13 and Fig. 14. As shown in these figures, the smooth dynamics motion is realized periodically.

5. Conclusion

The novel control method of bipedal control named Passive Dynamic Autonomous Control (PDAC) was proposed. PDAC is the method to take advantage of the robot

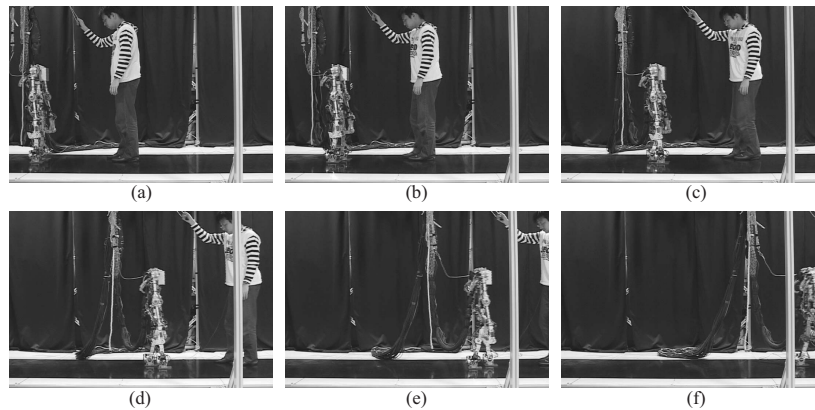


Fig. 12. Snapshots of the walking of PDAC. Each figure shows the snapshots at (a)1st (b)7th (c)12th (d)16th (e)19th (f)22th step.

inherent dynamics and realize natural dynamic walking. On the assumption that the sagittal and lateral motion can be separated and controlled individually, each motion was designed based on the given desired step-length and period. In order to stabilize walking, the landing position control according to the status was designed. In addition, the coupling method between these motions, which makes the period of each motion identical, was proposed. Finally, the 3-dimensional dynamic walking whose step-length is about 0.15[m] and velocity is about 0.23[m/s] was realized.

The proposed approach has the ability to stabilize walking against the disturbance. However, the effect of the modeling errors and sensing errors are not discussed in this paper. We just confirm that it is possible to realise 3D dynamic walking by means of proposed method. Thus, it is necessary to take these errors into consideration and prove the stability in the future.

References

1. A. Goswami, B. Espiau and A. Keramane, "Limit cycles in a passive compass gait baiped and passivity-mimicking control laws", *Autonomous Robots* 4, 1997, pp.274-286, Kluwer Academic Publishers.
2. A. D. Kuo, "Stabilization of Lateral Motion in Passive Dynamic Walking", *The International Journal of Robotics Research*, Vol. 18, No. 9, September 1999, pp. 917-930.
3. M. Raibert, "Legged Robots That Balance", MIT Press, 1986.
4. K. Nishiwaki, S. Kagami, Y. Kuniyoshi, M. Inaba and H. Inoue, "Online Generation of Humanoid Walking Motion based on a Fast Generation Method of Motion Pattern that Follows Desired ZMP" *The proceeding of the Int. Conf. Intelligent Robots and Systems*, 2002, pp. 2684-2689.
5. M. Vukobratovic, B. Brovac, D. Surla and D. Stokic, "Biped Locomotion:dynamics, stability, control, and application", Springer-Verlag, 1990.
6. A. Takanishi, M. Ishida, Y. Yamazaki and I. Kato, "The Realization of Dynamic Walking Robot WL-10RD", *The proceeding of Int. Conf. Advanced Robotics*, 1985,

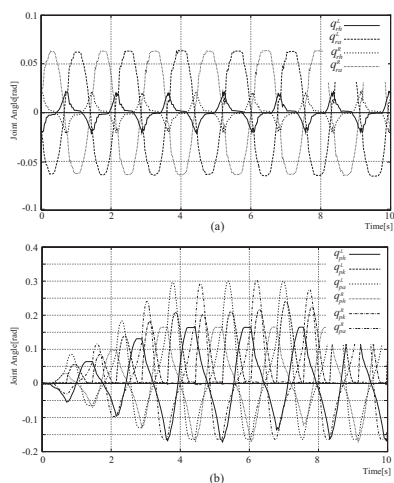


Fig. 13. Angle of the joints (a) in the lateral plane (b) in the sagittal plane

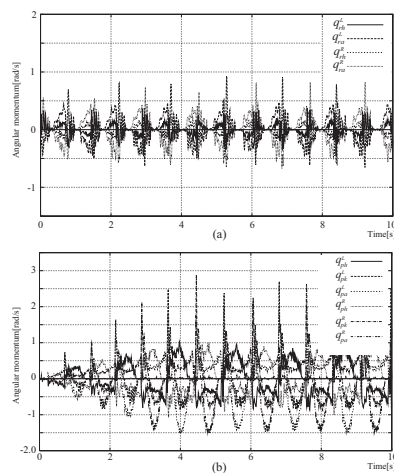


Fig. 14. Angular Velocity of the joints (a) in the lateral plane (b) in the sagittal plane

- pp. 459-466.
7. A. Sano and J. Furusho, "Realization of Dynamic Quadruped Locomotion in Pace Gait by Controlling Walking Cycle", International Symposium on Experimental Robotics, 1991, pp. 491-502.
 8. H. K. Khalil, "Nonlinear Systems", Prentice Hall, 3rd edition, 2001.
 9. H. Miura and I. Shimoyama, "Dynamic Walking of a biped", The International Journal of Robotics Research, Vol. 3, No. 2, 1984, pp. 60-74.
 10. J. W. Grizzle, G. Abba and F. Plestan, "Asymptotically Stable Walking for Biped Robots: Analysis via Systems with Impulse Effects", IEEE Transaction on Automatic Control, Vol. 46, No. 1, 2001, pp. 56-64.
 11. K. Hirai, M. Hirose, Y. Haikawa and T. Takenaka, "The Development of Honda Humanoid Robot", The proceeding of Int. Conf. Robotics and Automation, Vol. 2, 1998, pp. 1321-1326.
 12. S. Kajita, T. Yamaura and A. Kobayashi, "Dynamic walking control of a biped robot along a potential conserving orbit", IEEE Transactions on Robotics Automation, Vol. 8, No. 4, 1992, pp431-438.
 13. E. R. Westervelt, G. Buche and J. W. Grizzle, "Inducing Dynamically Stable Walking in an Underactuated Prototype Planar Biped", The proceeding of Int. Conf. Robotics and Automation, 2004, pp. 4234-4239.
 14. F. Plestan, J. W. Grizzle, E. R. Westervelt and G. Abba, "Stable Walking of a 7-DOF Biped Robot", IEEE Transactions on Robotics and Automation, Vol. 19, No. 4, August 2003, pp. 653-668.
 15. A. A. Grishin, A. M. Formal'sky, A. V. Lensky and S. V. Zhitomirsky "Dynamic Walking of a Vehicle With Two Telescopic Legs Controlled by Two Drives", The International Journal of Robotics Research, Vol. 13, No. 2, 1994, pp. 137-147.
 16. B. Thuijot, A. Goswami and B. Espiau, "Bifurcation and Chaos in a Simple Passive Bipedal Gait", The proceeding of Int. Conf. Robotics and Automation, 1997, pp. 792-798.

20 *Masahiro Doi, Yasuhisa Hasegawa, Toshio Fukuda*

17. M. Yamada, J. Furusho and A. Sano, "Dynamic control of walking robot with kick-action", The proceeding of the ICAR, 1985, pp. 405-412.
18. H. Hemami and B. F. Wyman, "Modeling and Control of Constrained Dynamic Systems with Application to Biped Locomotion in the Flontal Plane", IEEE Transactions on Automatic Control, Vol. AC-24, No. 4, August 1979, pp. 526-535.